Biologically modified microelectrode sensors provide enhanced sensitivity for detection of nucleic acid sequences from *Mycobacterium tuberculosis*

Ewen O. Blair [a],*, Stuart Hannah [a], Vincent Vezza [a], Hüseyin Avcı [b], Tanil Kocagoz [c], Paul A. Hoskisson [d], Fatma D. Güzel [e], Damion K. Corrigan [a]

[a] *Department of Biomedical Engineering, University of Strathclyde, 40 George Street, Glasgow G1 1QE, United Kingdom*
[b] *Department of Metallurgical and Materials Engineering & Cellular Therapy and Stem Cell Research Center, Eskişehir Osmangazi Üniversitesi, 26480 Eskişehir, Turkey*
[c] *Department of Medical Microbiology, Acibadem Mehmet Ali Aydinlar University, 34752 Istanbul, Turkey*
[d] *Strathclyde Institute of Pharmacy and Biomedical Sciences, University of Strathclyde, 161 Cathedral Street, Glasgow G4 0RE, United Kingdom*
[e] *Department of Biomedical Engineering, Ankara Yildirim Beyazit University, Kecioren, Ankara 06010, Turkey*

ARTICLE INFO

ABSTRACT

This paper describes improved sensitivity when using biosensors based on microfabricated microelectrodes to detect DNA, with the goal of progressing towards a low cost and mass manufacturable assay for antibiotic resistance in tuberculosis (TB). The microelectrodes gave an improvement in sensitivity compared to polycrystalline macroelectrodes. In addition, experimental parameters such as redox mediator concentration and experimental technique were investigated and optimised. It was found that lower concentrations of redox mediator gave higher signal changes when measuring hybridisation events and, at these lower concentrations, square wave voltammetry was more sensitive and consistent than differential pulse voltammetry. Together, this paper presents a quantifiable comparison of macroelectrode and microelectrode DNA biosensors. The final assay demonstrates enhanced sensitivity through reduction of sensor size, reduction of redox mediator concentration and judicious choice of detection technique, therefore maintaining manufacturability for incorporation into point of care tests and lab-on-a-chip devices.

1. Introduction

Tuberculosis (TB) was the number one global infectious disease killer in 2017 and results in an estimated 1.8 million deaths per year. Antibiotic resistance is becoming increasingly common in *Mycobacterium tuberculosis,* the aetiological agent of TB, with around half a million new rifampicin-resistant cases in 2018 [1]. Evidently, TB represents a significant public health risk. Delays in diagnosis, incorrectly prescribed drugs, and a failure to finish treatment courses in low and middle-income countries has exacerbated the emergence of multidrug resistant (MDR) and extremely drug resistant (XDR) strains of TB. The extent of this problem was highlighted by the World Health Organisation, who designated antibiotic resistant TB a "Critical Priority Pathogen" [2]. There is therefore a drive to develop new drugs and medical technologies to improve the situation. One vital stage in this process is the accurate diagnosis and assessment of the drug-resistance status of infections to ensure appropriate treatment is started as soon as possible. This is especially important in rural and low-income communities, where a lack of education and undernourishment lead to increased transmission and a worse prognosis [2–4].

Biosensors are a potential solution to this challenge, offering the ability to detect low concentrations of biomarkers in a very short time from a small sample. Many types of biosensors exist in literature and usually comprise a biological molecule coupled to a physical or chemical sensor. The molecule reacts to the presence of a biomarker and the sensor detects the change, such as from a binding or recognition event. This thereby generates a measurable signal when the biosensor comes into contact with the target of interest. There are many versions of this process, involving numerous sensor types and different bio-recognition elements. One which has been widely used is DNA, which has the advantage of being able to sense specific genetic sequences [5]. As well as this capacity to detect the presence of communicable and non-communicable illnesses such as TB, cancer, and sepsis, DNA based biosensors (also known as genosensors) are capable of profiling these to infer aspects of their phenotype including crucially, the presence of antibiotic resistance [6–8]. Popular sensing systems which are used in combination with DNA recognition include optical methods like surface plasmon resonance (SPR), Raman and surface-enhanced Raman spectroscopy (SERS), mechanical methods such as vibration of mechanical cantilevers, and electrochemical measurements [9–16]. Given the end goal of designing a diagnostic system which fulfils the criteria of being easily manufacturable, low cost and portable, electrochemical methods are particularly well suited. This is because they are generally smaller and

---

* Corresponding Author

feature simpler set-ups, with less dependence on expensive instrumentation [17–22]. However, their sensitivity generally needs improvement and many methods are commonly used to achieve this, include functionalising the electrode with nanoparticles, polymers, or graphene [23–25]. The disadvantage with these strategies is they make eventual mass manufacture of the sensor challenging, if not impossible. A route to achieving this is through microfabrication, which is responsible for the production of millions of nominally identical complex electronic components every year. Electrochemical sensors are frequently produced through microfabrication, since it enables fine control of features, integration with measurement electronics, and repeatable low-cost production [26–29]. It means it is not only feasible but desirable to produce electrodes with sizes on the micro-scale, as this conveniently improves their performance. Micro-scale electrodes are well established as having enhanced sensing properties over macro-scale electrodes, which results from their higher signal-to-noise ratio (SNR) [30–32]. These arise from the more efficient hemispherical diffusion that occurs at electrodes with a critical dimension smaller than their diffusion layer thickness, and yields a higher current density. The SNR is further improved by small electrodes having reduced capacitive charging currents relative to Faradaic currents and being less affected by electrical noise. Microfabricated microelectrodes are therefore an attractive and convenient method to improve biosensor sensitivity in a scalable and reliable manner. Surprisingly, given their advantages, only a relatively small proportion of biosensor studies utilise true microelectrodes and in particular, biologically modified ultramicroelectrodes [33, 34]. Of these studies, comparative studies of micro and macroelectrodes are very rare, which is unusual given the prevalence of literature quantifying the properties of microelectrodes as chemical sensors [31,35,36]. For example Slinker et al. briefly compared the two systems qualitatively using cyclic voltammetry of DNA functionalised electrodes [37]. A previous study including author DC demonstrated this improved sensitivity increased with decreasing size of microelectrode, but did not compare across the macro and microelectrode regimes [38]. In addition, other microelectrodes in literature have sensor enhancements which, although have yielded impressive sensitivity, impair manufacturability [39–41].

The microelectrodes presented in this study are a system capable of simple, mass production, with enhanced sensitivity conferred through the electrodes' size and reduction of the redox mediator concentration, with the goal of avoiding the use of exotic sensor enhancements. Their biosensing properties are also quantitatively compared against standard polycrystalline macroelectrodes by detecting specific TB DNA sequences. Firstly, the microelectrode fabrication and electrochemical characterisation are described. The electrochemical detection method is then improved by finding an optimal concentration of redox mediator and comparing square wave voltammetry (SWV) and differential pulse voltammetry (DPV). Using these improvements, microelectrodes are then compared with macroelectrodes in their ability to detect a complementary DNA target, mimicking a section of 16S rDNA from TB.

2. Materials and methods

2.1. Microelectrode fabrication

The microelectrodes were fabricated in the Institute of Photonics cleanroom facility at the University of Strathclyde on 100 mm Si wafers with a 1 μm-thick thermally grown SiO_2 insulation layer (University Wafer). The fabrication process is outlined in Fig. 1, and begins with sputtering a 100 nm Ti layer as an adhesion layer, followed by 150 nm of Au as in Fig. 1 (b). Next, a 600 nm-thick layer of SiO_2 was deposited using plasma enhanced chemical vapour deposition (PECVD) and patterned using photolithography to form a hard mask over the Au, which was subsequently etched. Following this, the hard mask was stripped as shown in Fig. 1 (c), leaving behind Au contact pads, interconnects, and electrodes. A 500 nm top insulator of PECVD SiO_2 was then deposited over the Au as in Fig. 1 (d). A layer of photoresist was patterned over the

top SiO_2 insulator, masking the wafer except for windows onto the SiO_2 where the contact pads and 30 μm diameter microelectrodes are formed. Those areas are then etched to expose the Au and the photoresist mask removed, which is shown in Fig. 1 (e). The wafer is the diced into individual devices, ready for use. A schematic of the finished device is presented in Fig. 1 (f).

2.2. Detection method

The detection principle of the biosensors in this paper is depicted in Fig. 1 (g)–(j) and begins with the attachment of a monolayer of single stranded DNA to the Au electrode. This is achieved through use of a thiol group attached to the 5' end of the DNA which binds semi-covalently to the Au. Measurements of the negatively charged potassium ferri and ferrocyanide redox couple are made before and after, with a decrease in signal meaning the redox molecules are hindered in their ability to reach the electrode and react, implying the surface is blocked by the DNA monolayer. When the electrode is incubated in a solution containing an oligonucleotide mimicking DNA from TB, based on the conserved 16S rDNA operon sequence [42], the oligonucleotide is able to hybridise with the DNA layer on the electrode surface. When remeasured in the same solution, even fewer of the redox molecules can reach the surface, as the DNA film is now denser, resulting in a further decrease of the signal. DPV and SWV were used to measure the ferri-ferrocyanide redox agent. These techniques have advantages over other commonly used methods like electrochemical impedance spectroscopy (EIS) since they are more relevant for the implementation of a point of care device, where generating AC frequencies and automated analysis of the response would be more complicated and expensive to deploy in the device instrumentation. Photographs showing the experimental set up are presented in figure S1 (a) and (b). Since Mycobacterium Tuberculosis bacteria are usually found in patient samples at a concentration of 10^8 or 10^9 cells per/mL or above, which is on the order of 100s of picomolar to the nanomolar range, this was the concentration range targeted [43].

2.3. Oligos and chemicals

Single-stranded oligonucleotides were purchased from Sigma Aldrich and the sequences are summarised in Table 1. The probe sequence was complementary to a conserved region of the 16S rDNA from *M. tuberculosis* while the target oligonucleotide mimicked this sequence. A non-complementary sequence was used to assess specificity. Mercapto-3-propanol (MCP), tris(2-carboxyethyl) phosphine (TCEP), potassium ferri and ferrocyanide, along with phosphate buffered saline (PBS) and sulphuric acid were also purchased from Sigma Aldrich. Deionised (DI) water was purchased from Scientific Laboratory Supplies. Polycrystalline Au electrodes purchased from Cambria Scientific were used for the macroelectrode measurements, with an Ag/AgCl reference electrode and Pt counter electrode, completing the three electrode set up. The details of these electrodes, along with photographs of the experimental set up can be found in the Supplementary Information. All potentials quoted are with respect to this reference electrode. The electrochemical measurements were performed on an Autolab (PGSTAT204, Metrohm-Autolab, Utrecht, Netherlands) potentiostat.

2.4. Electrode cleaning

Before all electrochemical measurements, the electrodes were cleaned according to the following procedure. Macroelectrodes were first polished with 0.3 μm alumina grit, followed by 0.05 μm alumina grit with intermediate rinses and 3-min sonications in DI water to prevent cross-contamination. Next they were soaked for 10 min in piranha solution comprising a 3:1 mix of sulphuric acid and hydrogen peroxide. Following this, cyclic voltammetry was performed on the electrodes in 100 mM sulphuric acid solution between the
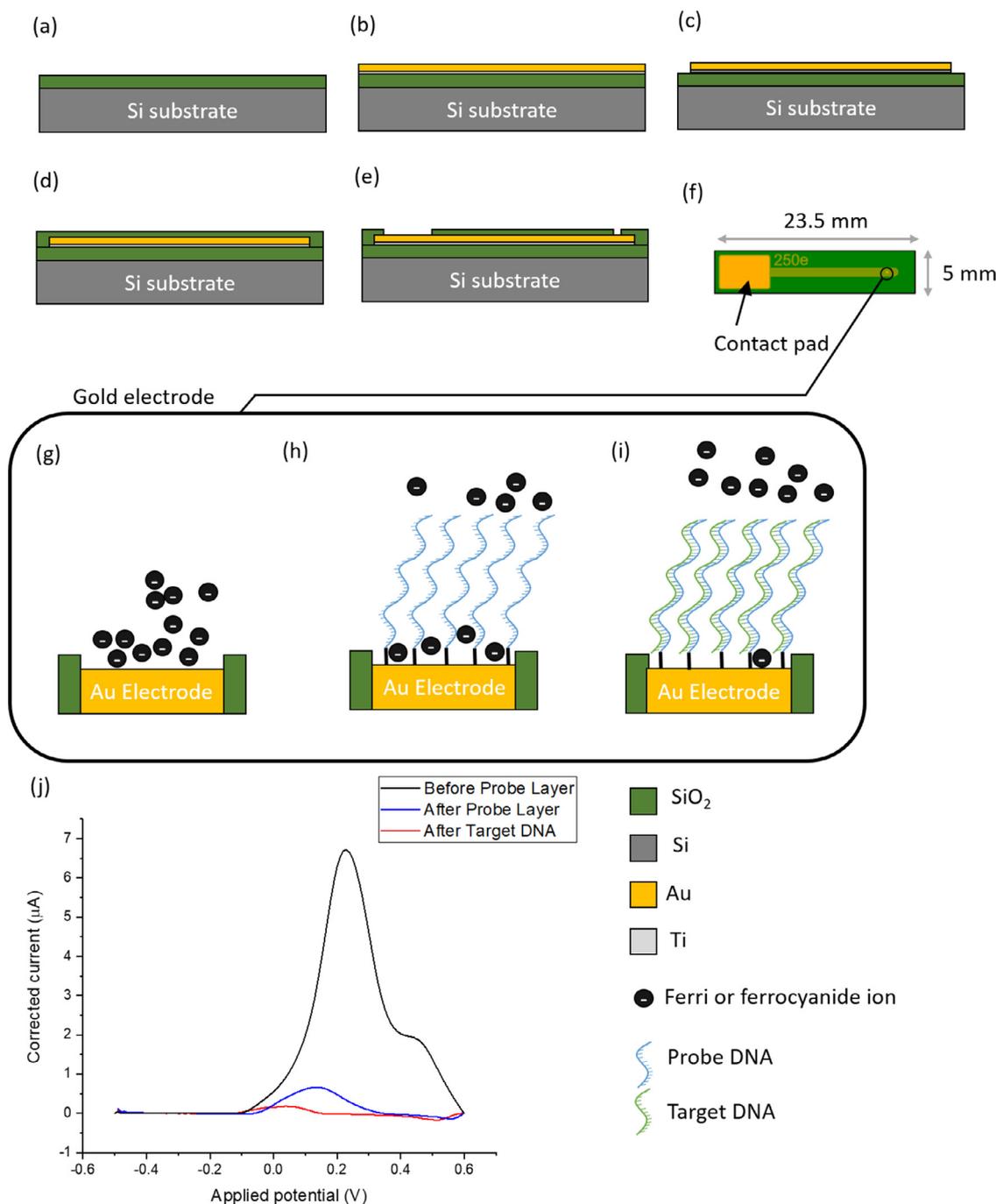
Fig. 1. Fabrication and detection process for the Au microelectrodes beginning with (a) a 100 mm Si wafer with a 1 μm layer of thermally grown SiO$_2$. (b) A layer 150 nm layer of Au is sputtered onto a 100 nm adhesion layer of Ti. (c) This layer is then patterned to form the contact pad and interconnect. (d) A 500 nm top passivation layer of PECVD SiO$_2$ is then deposited over the metal. (e) Windows are then etched into this top passivation, exposing the contact pad and microelectrode. (f) The finished sensor measuring ferri-ferrocyanide with (g) a blank Au electrode surface, (h) a layer of single stranded probe DNA bound to the Au surface repelling the ferri-ferrocyanide, (i) the probe DNA hybridised with target DNA blocking even more ferri-ferrocyanide, and (j) DPV scans taken at each of the three stages.

Table 1

Sequences used for the probe, complementary, and non-complementary target.

Role	Sequence
Probe sequence	[Thiol][SP16]CCACAAGACATGCATCCCG
Complementary sequence	CGGGATGCATGTCTTGTGGT
Non-Complementary sequence	

CCAAAGTGCAGGGCAGATCACCCACGTGTTACTCA

potentials −0.5 V and 1.75 V until the cyclic voltammograms (CVs) were unchanging. The electrodes were then rinsed in DI water before measurements were taken. The microelectrodes were cleaned by rinsing in DI water and drying in Ar gas before being cycled in 100 mM sulphuric acid between the same potentials as the macroelectrodes until the CV was stable. All measurements were performed in a solution of potassium ferri-ferrocyanide with a supporting electrolyte of 1 x PBS.
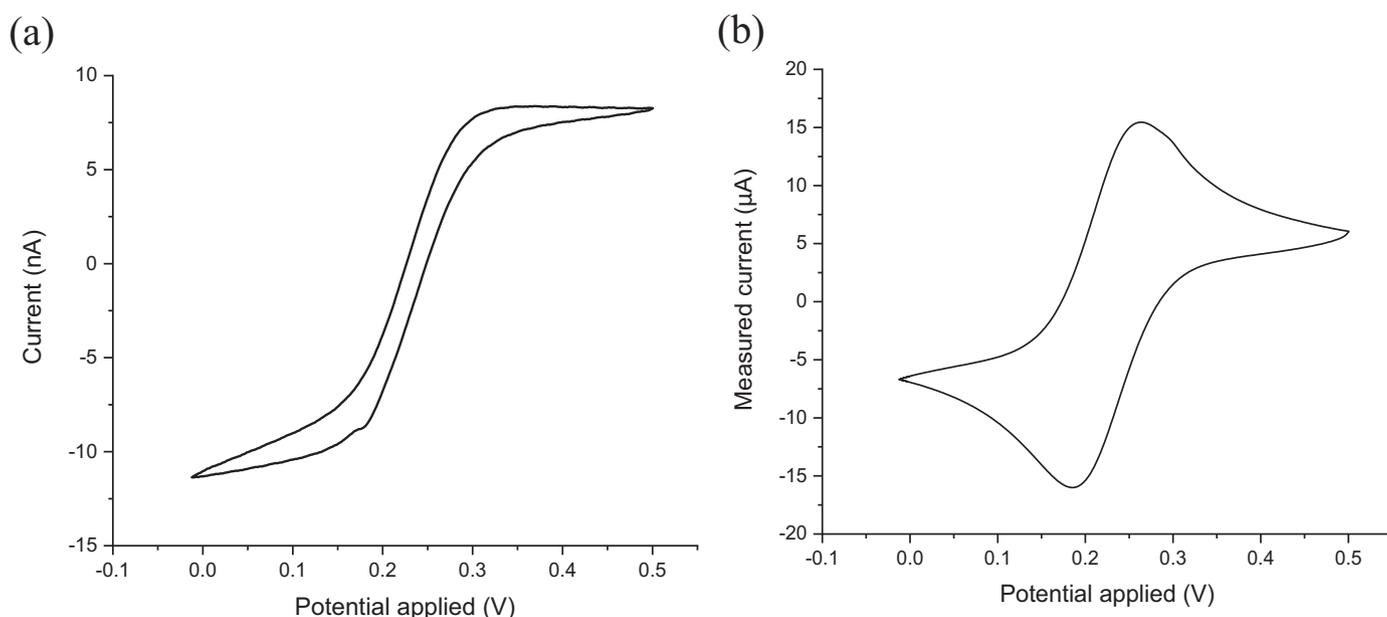
(a)

(b)

Fig. 2. (a) A cyclic voltammogram recorded on a 30 μm diameter microdisc electrode and (b) a cyclic voltammogram recorded on a gold macroelectrode, both in 2 mM ferri-ferrocyanide in a background of 1 x PBS at 50 mV/s.

2.5. Self-assembled monolayer (SAM) formation protocol

After initial measurements in ferri-ferrocyanide solution, both macro and microelectrodes were rinsed in DI water and dried under Ar before being incubated in a probe solution of 3 μM probe DNA with 15 μM TCEP in a background of 1 x PBS. The electrodes were left for 18−21 h at room temperature before being removed and rinsed for 10 s in DI water. The electrodes were then incubated in a backfilling solution which consisted of 1 mM MCP and 5 mM TCEP in 1 x PBS for one hour at room temperature to fill gaps in the probe DNA layer [44]. Following this, the electrodes were rinsed again in DI water for 10 s. For target incubations, the electrodes were incubated in a solution containing target DNA in 1 x PBS for one hour at room temperature. They were then rinsed in 5% PBS solution for 20 s.

3. Results

3.1. Macroelectrode and microelectrode electrochemical characterisation

In order to confirm that the fabricated microelectrodes were performing as expected, they were characterised by measuring the reduction and oxidation of potassium ferricyanide and ferrocyanide in free solution. Cyclic voltammetry (CV), differential pulse voltammetry (DPV), and square wave voltammetry (SWV) were then performed. Exemplar CV measurements are presented in Fig. 2 (a), compared with macroelectrode CV measurements recorded in the same solution in Fig. 2 (b). The characteristic wave-like shape, stereotypical of a microelectrode can be observed with a steady-state limiting current (i_L) in place of the peaks displayed by the macroelectrode. This limiting current is due to the extremely rapid establishment of diffusion-limited mass transport towards the microelectrode surface, resulting in a time independent steady state. Such a limiting current at a disc microelectrode of radius r, recessed by height L, can be quantified using Eq. (1) [45] below:

$$i_L = 4nFDcr\left(\frac{\pi r}{\pi r + 4L}\right) \tag{1}$$

where n is the number of electrons transferred in the reaction, F is Faraday's constant, D is the diffusion coefficient of the redox molecule, and c its concentration. The majority of microelectrodes were characterised in

a 1 mM solution of both ferri and ferrocyanide. When (1) is applied to this system, a theoretical value of 3.7 nA is obtained, using a diffusion coefficient of 6.67×10^{-10} m^2/s for both ferri- and ferrocyanide. This matches very closely the measured limiting current of 3.89 ± 0.56 nA from five devices. Although this confirms the successful production of microelectrodes, the limiting current is theoretically only dependant on radius of the microelectrode, whereas a consistent surface area is vital for measurements which employ a SAM. Therefore, the surfaces of both macroelectrodes and microelectrodes were characterised using atomic force microscopy (AFM) and scanning electron microscopy (SEM). The surface roughness (R_a) of the microelectrode gold was found to be 1.44 ± 0.3 nm and the surface showed far fewer defects than the macroelectrode (SEM and AFM scans of both electrode types are presented in Fig. S1). To further assess electrode consistency, DPV and SWV measurements were also performed. The peak heights were found to be 10.4 ± 1.21 nA for the DPV and 2.64 ± 0.31 nA for the SWV across five devices. The low variation between these separate devices, along with the predicted i_L, and relatively defect free surfaces with low roughness lend confidence that the surface area and geometry are as defined during the microfabrication. The current density was also assessed to determine if the microelectrodes were providing improved Faradaic signal over the macroelectrodes. This proved to be the case, as the current density for the oxidation of ferrocyanide at the microelectrodes was 5.5 ± 0.8 μA/ mm^2, compared with 0.854 ± 0.02 μA/mm^2 at the larger electrodes, across five devices each.

3.2. Optimisation of electrochemical detection

To optimise the detection process without further modifying the electrode surface through e.g. the addition of nanoparticles, additional parameters in the electrochemical measurement process were investigated. Previous studies in literature which employ ferri-ferrocyanide as a redox mediator usually work with concentrations between 1 and 10 mM and there does not seem to be a consensus as to which redox concentration yields the best sensing performance. To determine this for the setup presented here, measurements were performed in four ferri-ferrocyanide solutions of different concentration using Au macroelectrodes. Electrochemical measurements were made before and after probe formation, as well as after hybridisation with 500 nM solutions of complementary target. The four redox measurement solutions had concentrations of
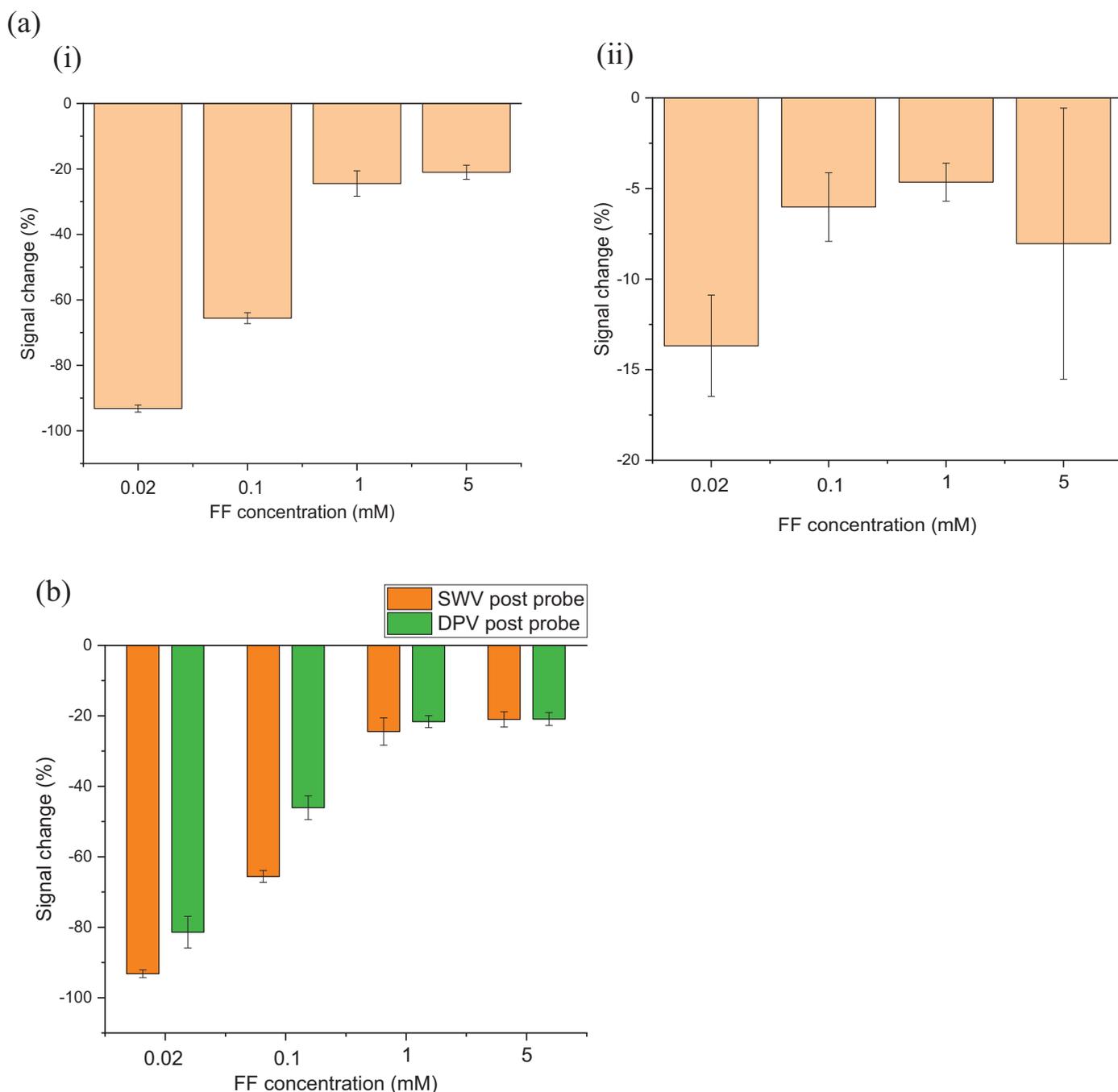
(a)

(i)

(ii)

(b)

Fig. 3. Signal change measured in different redox concentrations (a (i)) after probe layer formation and (a (ii)) after target hybridisation. (b) Signal change after probe layer formation, measured using both SWV and DPV. $N = 4$.

5 mM, 1 mM, 0.1 mM, and 0.02 mM ferri-ferrocyanide. Since previous measurements (unpublished data) had suggested that lower concentrations may prove to be more sensitive, the concentrations 0.1 mM and 0.02 mM were chosen as well as more commonly used values, 5 mM and 1 mM. Fig. 3 (a (i)) presents the signal change measured before and after forming the probe layer in all concentrations. A much larger signal change is evident in the dilute solutions, compared with the measurements made in 1 mM and 5 mM, which both exhibited similar decreases of 24% and 21%. The measurement in 0.02 mM gives the highest change of 93%. After hybridising with target DNA, as shown in Fig. 3 (a (ii)), this trend of increasing average signal change is also observed across the concentrations 0.02, 0.1, and 1 mM, although the high variation (as often seen in electrochemical DNA biosensors) means this is not statistically significant. The results suggest that lower concentrations of ferri-

ferrocyanide may yield higher signal changes for the sensor system presented in this study. However, there does not appear to be a body of evidence for any particular concentration, so further studies will be required. The origin of this is likely due to the original signal being lower, meaning when the decreases related to functionalisation or hybridisation occurs it represents a larger portion of the original signal.

To further understand the impact of the electrochemical measurement step, DPV and SWV were compared. Fig. 3 (b) compares the responses after probe formation, measured using SWV and DPV. For the higher concentrations, both the DPV and SWV show a similar signal change and variation level. However, for the lower concentrations, SWV yields both a higher signal change and a lower variation than DPV. SWV is known to be more sensitive than DPV, explaining its improved capacity to detect changes in low concentrations of analyte. It is therefore an
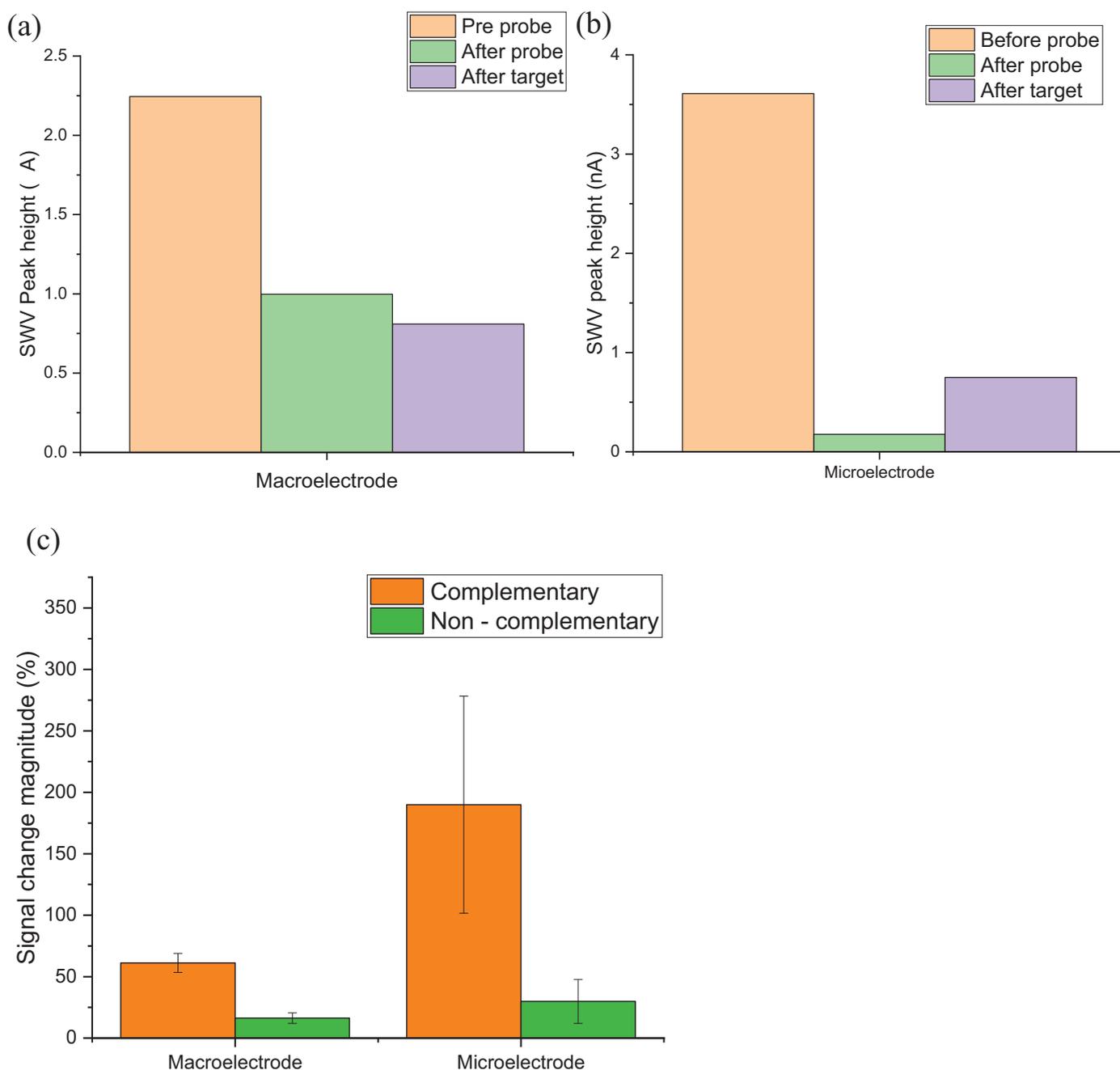
Fig. 4. SWV peak heights before probe layer functionalisation, after, and after target incubation on (a) a macroelectrode and (b) a microelectrode and (c) magnitude of signal change after hybridisation with complementary and non-complementary DNA on both systems, $N = 3$.

emerging technique for electrochemical biosensors [46,47]. This work is part of several which suggests that SWV may be important in the future of biosensor development and although there has been work in the area, aspects such as the frequency and pulse amplitude still require further investigation. SWV in a measurement solution of 0.02 mM was therefore used for the remainder of the measurements in this work.

To compare the response of the microelectrodes and macroelectrodes, measurements of 500 nM of fully complementary DNA were performed on both systems. Fig. 4 (a) shows exemplar data from a macroelectrode and (b) a microelectrode. Both electrodes show the expected decrease upon functionalising the surface with probe DNA and MCP. Upon hybridisation with target DNA, the macroelectrodes show a further decrease in signal as the target binds with probe and creates a denser layer of DNA, which physically and electrostatically hinders the ferri-ferrocyanide redox couple in reaching the surface. However, and

crucially, the signal from the microelectrodes was seen to increase after hybridisation. Such an effect has been observed in literature previously when carrying out bio-detection involving SAMs on micro-scale electrodes and is therefore not unexpected.

The performance of both systems was then compared when detecting the complementary and a non-complementary target, primarily with the aim of confirming sensor specificity. The responses are recorded in Fig. 4 (c), which compares the magnitude of the signal change on the microelectrodes and macroelectrodes when hybridised with 500 nM of each target. Firstly, both systems are able to distinguish between complementary and non-complementary target. Secondly, the microelectrodes demonstrate a much larger change in complementary signal than the macroelectrodes.

The last step of this initial characterisation was to establish a dose response trend and hence the sensitivity of the two systems. Fig. 5 (a)
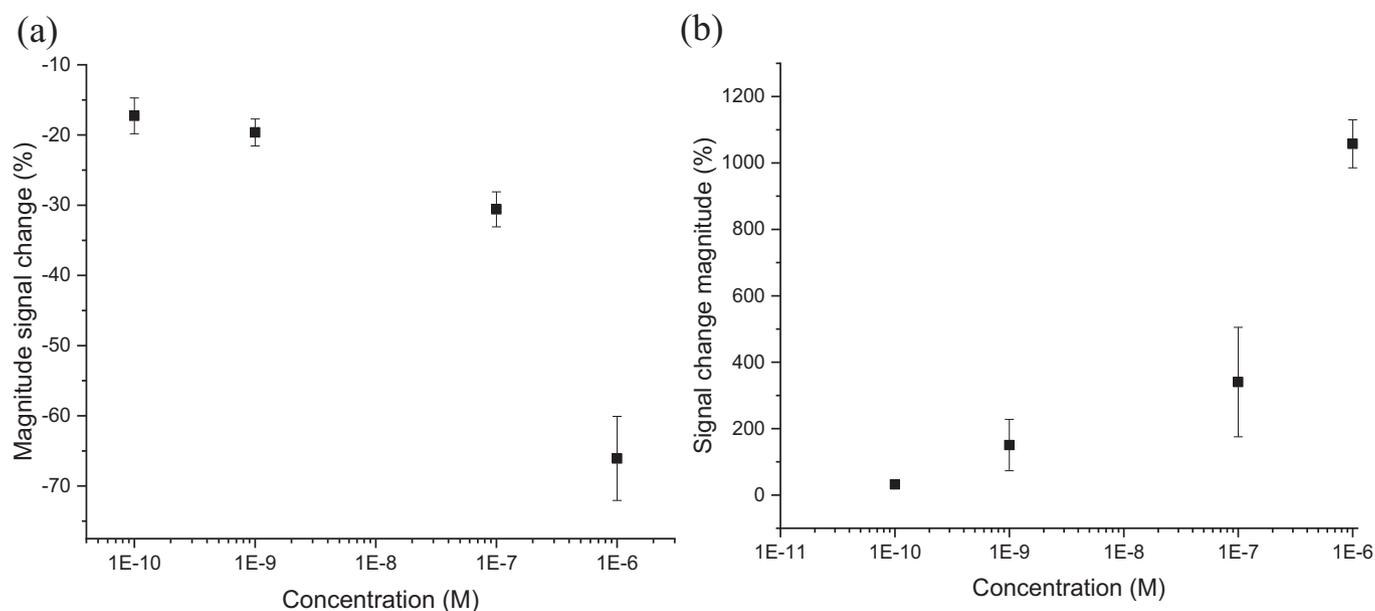
(a)

(b)

Fig. 5. Signal change measured in response to different concentrations of target DNA on (a) macroelectrodes and (b) microelectrodes. $N = 3$

shows the response of the macroelectrodes and (b) the microelectrodes to increasing concentrations of complementary target over a physiologically relevant range. The macroelectrodes exhibited the expected decrease in signal, which diminished with increasing concentration of target, while the microelectrodes demonstrated the opposite trend. The data were fitted using a function $Y = ax^b$, in order to capture the visually nonlinear trend, which stretched over the linear region and towards the saturation end of the sensor response. Using this function, a limit of detection (LoD) of 40 pM (Adj. R-square 0.991) was extracted for the microelectrodes. When applied to the macroelectrode data, the same expression yielded a LoD of 3.1 nM (Adj. R-square 0.978). This higher value is due to the variation in the baseline measurements of the macroelectrodes meaning that, although experimentally values lower than this were detected, they fell below the noise threshold of the sensor. This is interesting to note as the microelectrodes actually suffered from a slightly higher noise threshold due to their higher variability, but this was compensated for with their improved sensitivity and resulted in a much lower LoD than the macroelectrodes. What this also highlights is the variability present in biosensors in general, and is a challenge which has to be overcome in order to mass manufacture such devices.

The speed of response of the microelectrodes was also investigated through monitoring the SWV peak height over time and adding successive doses of complementary target. The average time for the peak height to stabilise after addition of target was 8 minutes and 45 s. Although the majority of additions stabilised in under 5 min, which can be seen in Fig. S3. It is also worth noting that the response time of the sensor will be highly dependent on the experimental set up used, as the time taken for the target to diffuse throughout the solution will depend on the volume and temperature of that solution, among other factors. Should such sensors be employed in a micro-reservoir or microfluidic set up, as we intend, the response time would likely be much faster owing to the improved diffusion of microchannels. From the wide range of concentrations chosen the detection range of the microelectrodes can at least be inferred to at least range from sub 100pM to above 1 μM, which covers the clinically relevant range under investigation.

This effect of increasing electrochemical signal for biological binding events when measured using microelectrodes or nanoelectrodes has been previously noted in literature and is hypothesised to be related to the behaviour of the DNA SAM on the electrodes surface [8,48,49]. It has been suggested that the single-stranded probe is coiled and blocks a larger portion of the electrode surface. When hybridised, a more rigid

duplex is formed pointing orthogonal to the electrode, therefore exposing more of the electrode surface and allowing more redox agent to react. This effect has been referred to as 'current gating'. Contrary to this, however, other examples of micro or nanoelectrode biosensor systems exist where the more standard decrease in signal has been observed [38,50]. Interestingly, Madina-Sanchez et al. fabricated novel rolled up microelectrodes and compared them with standard planar microelectrodes for measuring DNA hybridisation [51]. They found that the planar microelectrodes give an increase in charge transfer resistance, whereas the rolled up geometry recorded a decrease. One of the explanations put forward for this, was that the higher electric field within the tubular electrode compressed the ssDNA and subsequent hybridisation caused it to uncurl, exposing more of the electrode surface. It therefore seems that the signal change behaviour is not strictly tied to the size of the electrode, and may have more to do with the density, conformation, and composition of SAMs on small electrodes. It is clear that the formation of SAMs on micro-scale electrodes is an area which requires further investigation. Another effect seen in literature is the increase in the magnitude of signal change observed as electrode area decreases. This was again noted with the microelectrodes in this work, where they presented an average signal change of around 190% compared with the 66% change of the macroelectrodes after incubation with 500 nM target. This was reinforced by the concentration series presented in Fig. 5 which suggests the microelectrodes have a far lower LoD under these conditions than that of the macroelectrodes. Interestingly, this effect may not be bound to the electrochemical definition of a microelectrode as in literature many small electrodes, that are not micro by electrochemical standards, demonstrate improved sensitivity which is attributed to their size [52–54]. Finally, the variation in response was found to be higher for the microelectrodes as the error bars in Figs. 4 (c) and 5 (b) are larger for the microelectrodes. Despite the individual microelectrodes demonstrating higher sensitivity upon exposure to DNA target, device to device variation seemed to increase upon repeated hybridisations. The initial peak heights after incubating with probe DNA in Fig. 5 (b) were more consistent, with only 11% variation between devices. However, during the target measurements this increased with each subsequent incubation through 100 pM, 1 nM, and 100 nM. Although the final incubation of 1 μM did have a slightly lower variation than the previous two, it was still substantially higher than the macroelectrodes. Since the microelectrodes begin with a lower variation in peak height after formation of the probe layer, which is to be expected since the electrode geometries

proved consistent, it seems this might be an effect related to or exacerbated by repeated incubations and rinses. It was observed that when drying the microelectrodes after rinsing steps, it was difficult to retain a small amount of liquid on the surface in order to keep the DNA film hydrated, as the SiO_2 surface proved hydrophobic under these conditions. Despite this the microelectrodes successfully provided enhanced detection over the sensitivity range that Mycobacterium TB is present in sputum. Difficulties naturally remain in how to process real world sputum samples, which is a challenging matrix to work with [55]. This is a problem facing any TB detection assay and the work presented here forms one part of a larger project which is producing a lab on a chip system for diagnosing antibiotic resistance in TB. Although such sensors could be reused with the development of an adequate cleaning procedure, the nature of testing with clinical samples means, in reality, such sensing systems would likely be single use. In designing our sensors we have taken account of this and are able to produce high volumes of devices at low cost.

Another challenge in employing microelectrodes stems from the low currents measured. Currents were typically on the order of hundreds of picoamperes to single nanoamperes, and while this is readily measurable with a full lab-based potentiostat and electrical shielding, a low cost point of care device intended for use in the field will require careful engineering. Typically, in electrochemical systems, this shortcoming is circumvented by the use of arrays of microelectrodes which multiply the signal whilst benefitting from the enhanced microelectrode response. These are easily fabricated and several studies have demonstrated their applicability to biosensing [56]. Further work in this area is therefore required to (a) improve device performance consistency, (b) increase signal magnitude, and (c) further enhance sensitivity in a manner compatible with contemporary manufacturing processes.

3. Conclusions

This study has employed microfabricated microelectrodes to detect a nucleic acid sequence present in TB. The results represent an important contribution to the understanding of DNA biosensors based on the use of true microelectrodes. The DNA sequence employed was an uncomplicated linear probe, so complex and expensive hairpin structures were avoided and the operating conditions identified showed clear enhancement of signal from the microelectrode compared to standard polycrystalline macroelectrodes. The microelectrodes demonstrated a higher signal change in response to the complementary target and a lower LoD, although the response was more variable than the control macroelectrodes. Several other aspects of the detection process were optimised as well, including the concentration of the ferri-ferrocyanide redox mediator, which resulted in 0.02 mM being chosen, and the selection of SWV over DPV. This work presents a step towards an assay which is sensitive enough to be used for antibiotic susceptibility tests for TB, is low-cost, and is capable of mass production. Future work is to integrate this into a lab on a chip system and move towards working with real patient samples.

Declaration of Competing Interest

The authors declare that they have no known competing financial interests or personal relationships that could have appeared to influence the work reported in this paper.

Acknowledgements

Supplementary materials

Supplementary material associated with this article can be found in the online version at doi:10.1016/j.snr.2020.100008.

References

[1] W.H. Organisation, Global Tuberculosis Report 2019, United Nations, 2019, p. 297.

[2] W.H. Organisation, Prioritization of pathogens to guide discovery, research and development of new antibiotics for drug resistant bacterial infections, including tuberculosis, Online2017.

[3] A. Bhargava, M. Chatterjee, Y. Jain, B. Chatterjee, A. Kataria, M. Bhargava, et al., Nutritional status of adult patients with pulmonary tuberculosis in rural central India and its association with mortality, PLoS One 8 (2013).

[4] N.R. Gandhi, P. Nunn, K. Dheda, H.S. Schaaf, M. Zignol, D. van Soolingen, et al., Multidrug-resistant and extensively drug-resistant tuberculosis: a threat to global control of tuberculosis, Lancet 375 (2010) 1830–1843.

[5] E.O. Blair, D.K. Corrigan, A review of microfabricated electrochemical biosensors for DNA detection, Biosens. Bioelectron. 134 (2019) 57–67.

[6] V.C. Diculescu, A.-M.C. Paquim, A.M.O. Brett, Electrochemical DNA sensors for detection of DNA damage, Sensors 5 (2005) 377–393.

[7] M. Liu, A. Khan, Z. Wang, Y. Liu, G. Yang, Y. Deng, et al., Aptasensors for pesticide detection, Biosens. Bioelectron. 130 (2019) 174–184.

[8] C. Russell, A.C. Ward, V. Vezza, P. Hoskisson, D. Alcorn, D.P. Steenson, et al., Development of a needle shaped microelectrode for electrochemical detection of the sepsis biomarker interleukin-6 (IL-6) in real time, Biosens. Bioelectron. 126 (2019) 806–814.

[9] J.L. Arlett, E.B. Myers, M.L. Roukes, Comparative advantages of mechanical biosensors, Nat. Nanotechnol. 6 (2011) 203–215.

[10] J. Homola, Present and future of surface plasmon resonance biosensors, Anal. Bioanal. Chem. 377 (2003) 528–539.

[11] J. Wang, Electroanalysis and biosensors, Anal. Chem. 71 (1999) 328–332.

[12] H.T. Ngo, H.-N. Wang, A.M. Fales, T. Vo-Dinh, Plasmonic SERS biosensing nanochips for DNA detection, Anal. Bioanal. Chem. 408 (2015) 1773–1781.

[13] O.S. Wolfbeis, Fiber-optic chemical sensors and biosensors, Anal. Chem. 80 (2008) 4269–4283.

[14] H. Šípová, J. Homola, Surface plasmon resonance sensing of nucleic acids: a review, Anal. Chim. Acta 773 (2013) 9–23.

[15] F.D. Guzel, H. Avci, Fabrication of nanopores in an ultra-thin polyimide membrane for biomolecule sensing, IEEE Sens. J. 18 (2018) 2641–2646.

[16] F.D. Güzel, B. Miles, Development of in-flow label-free single molecule sensors using planar solid-state nanopore integrated microfluidic devices, Micro Nano Lett. Inst. Eng. Technol. (2018) 1352–1357.

[17] A. Butterworth, D.K. Corrigan, A.C. Ward, Electrochemical detection of oxacillin resistance with SimpleStat: a low cost integrated potentiostat and sensor platform, Anal. Methods 11 (2019) 1958–1965.

[18] T.G. Drummond, M.G. Hill, J.K. Barton, Electrochemical DNA sensors, Nat. Biotechnol. 21 (2003).

[19] D. Grieshaber, R. MacKenzie, J. Vörös, E. Reimhult, Electrochemical biosensors - sensor principles and architectures, Sensors 8 (2008) 1400–1458.

[20] S. Libertino, S. Conoci, A. Scandurra, C. Spinella, Biosensor integration on Si-based devices: feasibility studies and examples, Sens. Actuators B 179 (2013) 240–251.

[21] F.D. Guzel, Development of an on-chip antibiotic permeability assay with single molecule detection capability, IEEE Trans. NanoBiosci. 17 (2018) 155–160.

[22] S. Hannah, E. Addington, D. Alcorn, W. Shu, P.A. Hoskisson, D.K. Corrigan, Rapid antibiotic susceptibility testing using low-cost, commercially available screen-printed electrodes, Biosens. Bioelectron. 145 (2019) 111696.

[23] J.M. George, A. Antony, B. Mathew, Metal oxide nanoparticles in electrochemical sensing and biosensing: a review, Microchim. Acta 185 (2018).

[24] S. Kumar, W. Ahlawat, R. Kumar, N. Dilbaghi, Graphene, carbon nanotubes, zinc oxide and gold as elite nanomaterials for fabrication of biosensors for healthcare, Biosens. Bioelectron. 70 (2015) 498–503.

[25] W. Yang, K.R. Ratinac, S.P. Ringer, P. Thordarson, J.J. Gooding, F. Braet, Carbon nanomaterials in biosensors: should you use nanotubes or graphene? Angew. Chem. Int. Ed. 49 (2010) 2114–2138.

[26] R. Feeney, S.P. Kounaves, Microfabricated ultramicroelectrode arrays: developments, advances, and applications in environmental analysis, Electroanalysis 12 (2000) 677–684.

[27] M.E. Gray, J.R.K. Marland, C. Dunare, E.O. Blair, J. Meehan, A. Tsiamis, et al., In vivo validation of a miniaturized electrochemical oxygen sensor for measuring intestinal oxygen tension, Am. J. Physiol.-Gastrointest. Liver Physiol. 317 (2019) G242–GG52.

[28] J.R.K. Marland, E.O. Blair, B.W. Flynn, E. González-Fernández, L. Huang, I.H. Kunkler, et al., in: S. Mitra, D. Cumming (Eds.), Springer, Cham, 2018, pp. 259–286.

[29] J. Wang, Survey and summary: from DNA biosensors to gene chips, Nucleic Acids Res. 28 (2000) 3011–3016.

[30] A.J. Bard, L.R. Faulkner, Electrochemical Methods: Fundamentals and Applications, Wiley, 2001.

[31] D.K. Corrigan, E.O. Blair, J.G. Terry, A.J. Walton, A.R. Mount, Enhanced electroanalysis in lithium potassium eutectic (LKE) using microfabricated square microelectrodes, Anal. Chem. 86 (2014) 11342–11348.

[32] R.J. Forster, Microelectrodes: new dimensions in electrochemistry, Chem. Soc. Rev. 23 (1994) 289–297.

[33] E. Baldrich, F.J. del Campo, F.X. Muñoz, Biosensing at disk microelectrode arrays. Inter-electrode functionalisation allows formatting into miniaturised sensing platforms of enhanced sensitivity, Biosens. Bioelectron. 25 (2009) 920–926.

[34] I. Fritsch, Z.P. Aguilar, Advantages of downsizing electrochemical detection for DNA assays, Anal. Bioanal. Chem. 387 (2007).

[35] R. John, G.G. Wallace, The use of microelectrodes as substrates for chemically modified sensors: a comparison with conventionally sized electrodes, J. Electroanal. Chem. Interfacial Electrochem. 283 (1990) 87–98.

[36] X. Dai, G.G. Wildgoose, C. Salter, A. Crossley, R.G. Compton, Electroanalysis using macro-, micro-, and nanochemical architectures on electrode surfaces. Bulk surface modification of glassy carbon microspheres with gold nanoparticles and their electrical wiring using carbon nanotubes, Anal. Chem. 78 (2006) 6102–6108.

[37] J.D. Slinker, N.B. Muren, A.A. Gorodetsky, J.K. Barton, Multiplexed DNA-modified electrodes, J. Am. Chem. Soc. 132 (2010) 2769–2774.

[38] P. Quan Li, A. Piper, I. Schmueser, A.R. Mount, D.K. Corrigan, Impedimetric measurement of DNA–DNA hybridisation using microelectrodes with different radii for detection of methicillin resistant Staphylococcus aureus (MRSA), Analyst 142 (2017) 1946–1952.

[39] J. Das, I. Ivanov, T.S. Safaei, E.H. Sargent, S.O. Kelley, Combinatorial probes for high-throughput electrochemical analysis of circulating nucleic acids in clinical samples, Angew. Chem. Int. Ed. 57 (2018) 3711–3716.

[40] M. Barbaro, A. Caboni, D. Loi, S. Lai, A. Homsy, P.D. van der Wal, et al., Label-free, direct DNA detection by means of a standard CMOS electronic chip, Sens. Actuators B 171–172 (2012) 148–154.

[41] P.E. Lobert, D. Bourgeois, R. Pampin, A. Akheyar, L.M. Hagelsieb, D. Flandre, et al., Immobilization of DNA on CMOS compatible materials, Sens. Actuators B 92 (2003) 90–97.

[42] M.C. Menendez, M.J. Garcia, M.C. Navarro, J.A. Gonzalez-y-Merchand, S. Rivera-Gutierrez, L. Garcia-Sanchez, et al., Characterization of an rRNA Operon (rrnB) of Mycobacterium fortuitum and Other Mycobacterial Species: Implications for the Classification of Mycobacteria, J. Bacteriol. 184 (2002) 1078.

[43] S.O. Kelley, What are clinically relevant levels of cellular and biomolecular analytes? ACS Sens. 2 (2017) 193–197.

[44] A. Butterworth, E. Blues, P. Williamson, M. Cardona, L. Gray, D.K. Corrigan, SAM composition and electrode roughness affect performance of a DNA biosensor for antibiotic resistance, Biosensors 9 (2019).

[45] A.M. Bond, D. Luscombe, K.B. Oldham, C.G. Zoski, A comparison of the chronoamperometric response at inlaid and recessed disc microelectrodes, J. Electroanal. Chemi. Interfac. Electrochem. 249 (1988) 1–14.

[46] A. Chen, B. Shah, Electrochemical sensing and biosensing based on square wave voltammetry, Anal. Methods 5 (2013) 2158–2173.

[47] P. Dauphin-Ducharme, K.W. Plaxco, Maximizing the signal gain of electrochemical-DNA sensors, Anal. Chem. 88 (2016) 11654–11662.

[48] G. Liu, C. Sun, D. Li, S. Song, B. Mao, C. Fan, et al., Gating of redox currents at gold nanoelectrodes via DNA hybridization, Adv. Mater. 22 (2010) 2148–2150.

[49] P. Jolly, N. Formisano, J. Tkáč, P. Kasák, C.G. Frost, P. Estrela, Label-free impedimetric aptasensor with antifouling surface chemistry: a prostate specific antigen case study, Sens. Actuators B 209 (2015) 306–312.

[50] A. Piper, Ben M. Alston, D.J. Adams, A.R. Mount, Functionalised microscale nanoband edge electrode (MNEE) arrays: the systematic quantitative study of hydrogels grown on nanoelectrode biosensor arrays for enhanced sensing in biological media, Faraday Discuss. 210 (2018) 201–217.

[51] M. Medina-Sánchez, B. Ibarlucea, N. Pérez, D.D. Karnaushenko, S.M. Weiz, L. Baraban, et al., High-performance three-dimensional tubular nanomembrane sensor for DNA detection, Nano Lett. 16 (2016) 4288–4296.

[52] L. Anorga, A. Rebollo, J. Herran, S. Arana, E. Bandres, J. Garcia-Foncillas, Development of a DNA microelectrochemical biosensor for CEACAM5 detection, IEEE Sens. J. 10 (2010) 1368–1374.

[53] S. Petralla, F. Rundo, S. Conoci, M.L.D. Pietro, E.L. Sciuto, S. Mirabella, Electrochemical biosensor for PCR free nucleic acids detection: A novel biosensor containing three planar microelectrodes for melocular diagnostic applications, 2017 European Conference on Circuit Theory and Design (ECCTD), 2017, pp. 1–4.

[54] A.L. Ghindilis, K. Schwarzkopf, D. Messing, I. Sezan, P. Schuele, C. Zhan, et al., Real-time biosensor platform: fully integrated device for impedimetric assays, ECS Trans. 33 (2010) 59–68.

[55] R. McNerney, M. Maeurer, I. Abubakar, B. Marais, T.D. Mchugh, N. Ford, et al., Tuberculosis diagnostics and biomarkers: needs, challenges, recent advances, and opportunities, J. Infect. Dis. 205 (2012) S147–SS58.

[56] R. Hintsche, M. Paeschke, U. Wollenberger, U. Schnakenberg, B. Wagner, T. Lisec, Microelectrode arrays and application to biosensing devices, Biosens. Bioelectron. 9 (1994) 697–705.